

# **COUPLING GEOMECHANICS AND RESERVOIR MODELS : APPLICATION TO THE ROLE OF FRACTURES AND FAULTS**

**Marc Mainguy, Applied Mechanics Division, IFP – France,  
Nick Koutsabeloulis, VIPS (Vector International Processing Systems) Ltd,  
Winkfield-Windsor, Berkshire, UK,  
& Pascal Longuemare, Applied Mechanics Division, IFP – France.**

## **Abstract**

Faults and fractures play a significant role in the mechanical and hydraulic behaviour of hydrocarbon reservoirs. This paper investigates these effects for a reservoir of simplified geometry using the stress dependent reservoir simulator ATH2VIS that makes the coupling of the reservoir simulator ATHOS<sup>TM</sup> developed at IFP with the stress simulator VISAGE<sup>TM</sup> developed by VIPS. The partial coupling between the reservoir and stress simulators relies on the computation of the stress state of the reservoir and the adjacent formations induced by reservoir pressure and thermal variations. Using these variations as loading condition, VISAGE<sup>TM</sup> predicts the rock strains and fracturing induced through fractures and faults, which lead to a modification of the reservoir permeability.

Sensitivity of reservoir simulation to geomechanical effects is tested on a three-dimensional test problem with a dead-oil. Simulations realised with a fault in the reservoir show significant modifications of the stress state around the fault, which may cause a threat to well integrity. Nevertheless, the fault being initially described as a very low permeable zone in the reservoir simulator, the stress state variation around the fault does not significantly alter the flow in the reservoir. On the contrary, other simulations considering fractures in the reservoir reveal significant variations of the permeability around water injection wells, which in turn modify the simulation results of the reservoir simulator.

## **Introduction**

Hydrocarbon reservoir production induces significant variations in time and space of reservoir pressures and temperatures, which may cause for stress sensitive reservoir a modification of the stress state in and around the reservoir. The stress changes may in turn:

- alter the reservoir properties such as porosity and permeability, and then flows within the reservoir and the reservoir productivity,
- cause a threat to well integrity when the change in stress state leads to significant ground strains around wells.

These effects result from the coupling between geomechanics and reservoir fluid flow, and can be analysed with coupled multiphase hydro-thermo-mechanical simulators. During the last twenty years such coupled simulators have been developed to investigate the effects of reservoir compaction (See e.g. Settari and Mourits, 1994; Chin and Thomas, 1999), reservoir stress dependent permeability (see e.g. Chin et al., 1998), and fracture permeability variation of fractured reservoir (see e.g. Gutierrez and Makurat, 1997).

This paper presents simulation results of a new stress dependent reservoir simulator ATH2VIS that makes the coupling of the reservoir simulator ATHOS<sup>TM</sup> developed at IFP with the stress simulator VISAGE<sup>TM</sup> developed by VIPS. This first version of ATH2VIS is a reservoir stress dependent permeability model. It accounts for permeability variations due to activation of fractures and faults together with rock failure. Two simulation cases are presented for a 3-D reservoir of idealised rectangular geometry, which illustrate the role of faults and fractures on the stress state change and on the reservoir productivity.

## **ATH2VIS: a stress dependent reservoir simulator**

Following the definition of Settari and Mourits (1994), ATH2VIS is a partially coupled simulator using the standard reservoir simulator ATHOS<sup>TM</sup> in conjunction with the standard finite element stress analysis code VISAGE<sup>TM</sup>. As outlined by the previous authors, the partial coupling has the advantage of being flexible and computing cost effective compared to a fully coupled solver based on the simultaneous resolution of the complete hydro-thermo-mechanical equations. Furthermore, it also benefits from the high developments in physics and numerical techniques of both the reservoir simulator and the mechanical software:

- ATHOS<sup>TM</sup> is a multi-purpose, fully compositional reservoir simulator that integrates several simulation models within a single and consistent framework. ATHOS<sup>TM</sup> incorporates a suite of simulation options allowing engineers to enhance and specialise the reservoir model, from black-oil to compositional simulation, combined with thermal modelling or dual porosity/dual permeability option for fractured reservoir. ATHOS<sup>TM</sup> offers cost-effective solution to reservoir engineers and a unique data preparation and management tool with the database management environment SimView developed by Beicip-Franlab.
- VISAGE<sup>TM</sup> is one of the most advanced and comprehensive stress analysis simulators commercially available. It has been developed for applications where non-linear mechanics are more profound and commonly met such as in geotechnics and rock mechanics. It is flexible and can also be applied to many other scientific disciplines, such as fluid flow mechanics, heat transfer, materials science etc. The system offers computational power and modelling sophistication to many analytical situations, which currently include mining, civil engineering and reservoir engineering.

The coupling between ATHOS<sup>TM</sup> and VISAGE<sup>TM</sup> is based on the updating of reservoir permeability values with stress dependent permeability values computed with VISAGE<sup>TM</sup>. Permeability updating occurs at user's prescribed times and there is no iterated process between each simulator on a common time period. Fig. 1 illustrates the procedure of partial coupling between the reservoir simulator ATHOS<sup>TM</sup> and the stress code VISAGE<sup>TM</sup>:

- At defined times values, pore pressure and temperature changes computed by the reservoir simulator are converted in distributed load in the stress simulator.
- Applying the distributed loads, stress analysis performed on the reservoir and the possible adjacent formations provides the rock strains and fracturing. The stress analysis uses viscoplastic algorithm to predict the onset of fracturing of the rock mass behaving as an 'equivalent material' (see Koutsabeloulis et al., 1994). For an 'equivalent material', the 'intact' rock is modelled separately from the joints, which in turn are modelled using the concept of the multi-laminate theory of Pande (1980).
- Using permeability sensitive laws described in Koutsabeloulis and Hope (1998), VISAGE<sup>TM</sup> computes new permeability for reservoir cells where fracturing occurs through fractures and faults and where the intact rock fails alone. Permeability sensitive laws mainly account for the enhancement of the permeability with the normal strain to the

fracture and the reduction of the permeability with the shear strain in the transverse direction of the fracture.

- Reservoir simulator reads the stress dependent permeability values and restarts the reservoir simulation until the next meeting time with the stress simulator.

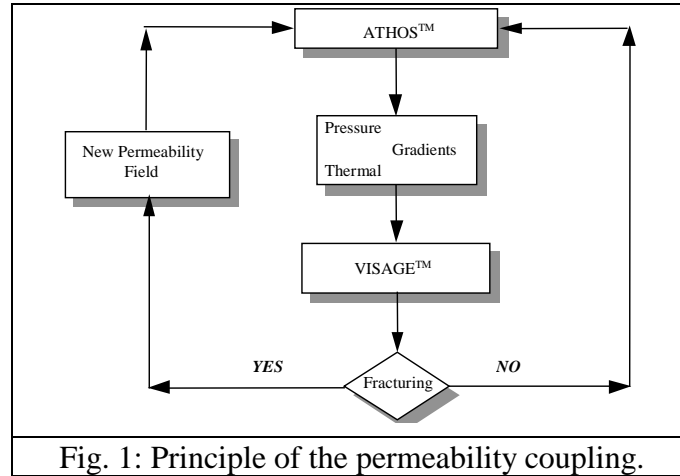


Fig. 1: Principle of the permeability coupling.

### An Idealised Model:

Fig. 2 displays an idealised reservoir mesh (Corner Point Geometry) used for ATHOS™ simulations. It is 1500 m by 1500 m large with a vertical depth of 150 m. VISAGE™ finite element mesh is constituted with the reservoir geometry, an overburden going from 0 to 2500 m, an underburden going from 2650 m to 3300 m, and sideburden. Thus the total dimensions of the stress mesh are 7500 m by 7500 m for a total height of 3300 m (see Fig. 3).

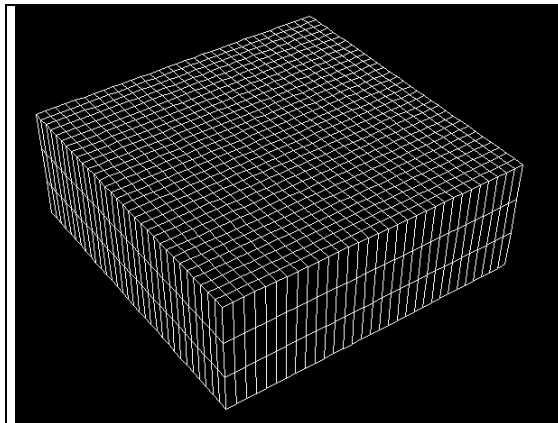


Fig. 2: ATHOS™ reservoir mesh (31×31×3 blocks)

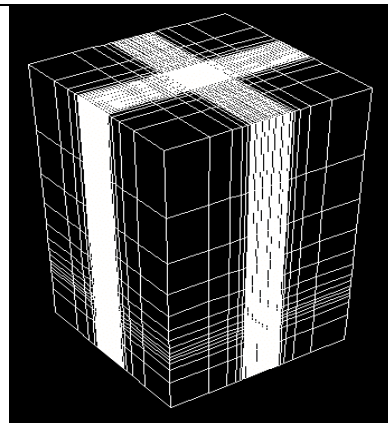


Fig. 3: VISAGE™ reservoir and adjacent formations mesh (41×41×14 blocks)

Reservoir simulations are performed with a dead oil and a thermal option. Reservoir fluid flow and thermal properties are mainly given in Table 1, except for PVT data and relative permeability functions not presented in the paper. Note that the relative permeability functions are defined with an irreducible water saturation of 0.3 that approximately corresponds to the initial water saturation in the reservoir. Mechanical parameters used for the reservoir and the adjacent formations (overburden, underburden and sideburden) are given in Tables 2 and 3. Tables 2 and 3 also provide the parameters of the Coulomb criterion used to describe the non-linear behaviour of the rocks. Note that the high values used for the cohesion and tensile stress

ensure that fracturing is only induced through fault and joint sets, but not with the intact rock failure. The initial stress state for the mechanical mesh is defined with the effective vertical stress in the reservoir and the ratios of the maximal and minimal effective horizontal stress with the vertical one. In the present case, these ratios equal 0.8 and 0.4 and the minimal horizontal stress is aligned with the x direction. Finally, boundary conditions applied to the mechanical mesh are a null loading on the upper overburden boundary and null displacements on the remaining boundaries.

Table 1: Reservoir properties.

Porosity	0.10 (-)
Vertical permeability	1 md
Horizontal permeability	10 md
Net to gross	1
Pore compressibility	$6 \cdot 10^{-5} \text{ bar}^{-1}$
Initial temperature	85 C
Volumetric heat capacity	2 J/cm <sup>3</sup> .K
Thermal conductivity	2 W/m.K

Table 2: Reservoir mechanical parameters.

Young's modulus	$3 \cdot 10^5 \text{ bar}$
Poisson's ratio	0.2
Cohesion	high
Friction angle	30 deg
Dilation angle	5 deg
Tensile stress	high
Biot constant	0.6
Thermal expansion coefficient	$1.6 \cdot 10^{-4} \text{ C}^{-1}$
Specific gravity	2.2

Table 3: Adjacent formation mech. parameters.

Young's modulus	$3 \cdot 10^4 \text{ bar}$
Poisson's ratio	0.3
Cohesion	high
Friction angle	30 deg
Dilation angle	5 deg
Tensile stress	high
Biot constant	1.0
Thermal expansion coefficient	$1.6 \cdot 10^{-4} \text{ C}^{-1}$
Specific gravity	2.2

The next sections present simulation results performed on the idealised geometry with the stress dependent simulator ATH2VIS and the standard reservoir simulator ATHOS<sup>TM</sup>. The first stress dependent simulation uses joint sets whereas the second one is realised with a fault of reduced permeability.

Table 4: Fault parameters.

Young's modulus	$7 \cdot 10^3 \text{ bar}$
Dip	90 deg
Normal stiffness	$1 \cdot 10^5 \text{ bar/m}$
Shear stiffness	$4 \cdot 10^4 \text{ bar/m}$
Friction angle	20 deg
Dilation angle	10 deg

Table 5: Joint parameters.

Dip	90 deg
Dip direction	60/120 deg
Normal stiffness	$2 \cdot 10^6 \text{ bar/m}$
Shear stiffness	$1 \cdot 10^6 \text{ bar/m}$
Friction angle	20 deg
Dilation angle	10 deg
Spacing	5 m

## Role of fractures

In order to study the role of fractures on fluid flows on the reservoir, this section compares a reservoir simulation performed with ATHOS<sup>TM</sup> with a stress dependent simulation performed with ATH2VIS and where two joint sets are inserted in the mechanical model. Table 5 displays joint set characteristics used for the stress analysis. Vertical fractures are oriented with a dip direction of 60 and 120 degrees that corresponds to fractures oriented of + or - 30 degrees with respect to the direction of horizontal maximal stress.

The production scenario consists of a 1-year natural depletion of the reservoir followed by cold water injection until the producer bottom hole pressure reaches a threshold value. Reservoir field is constituted with one producer well P1 located at the centre of the reservoir

(cell 16\*16 in Fig. 2), and 4 cold water (20 C) injector wells (I1 to I4) approximately located at the centre of a quadrant of the reservoir (cells 9/23\*9/23 in Fig. 2). Central well produces oil and water at surface condition imposed to 500 m<sup>3</sup>/d, and its production stops when bottom hole pressures reaches 70 bar. Cold water injectors inject water at a flow rate fixed to 125 m<sup>3</sup>/d at surface condition.

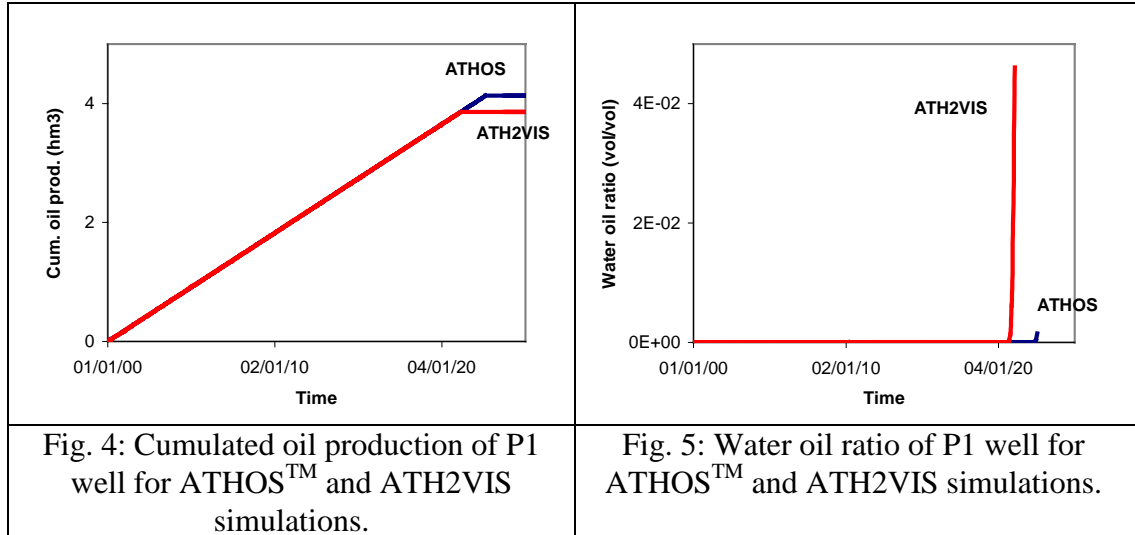
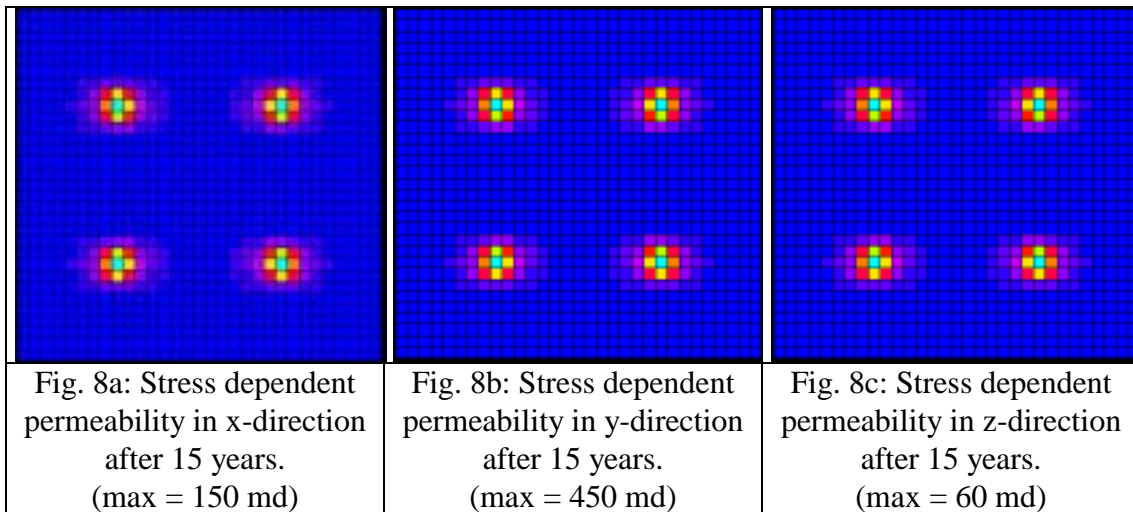
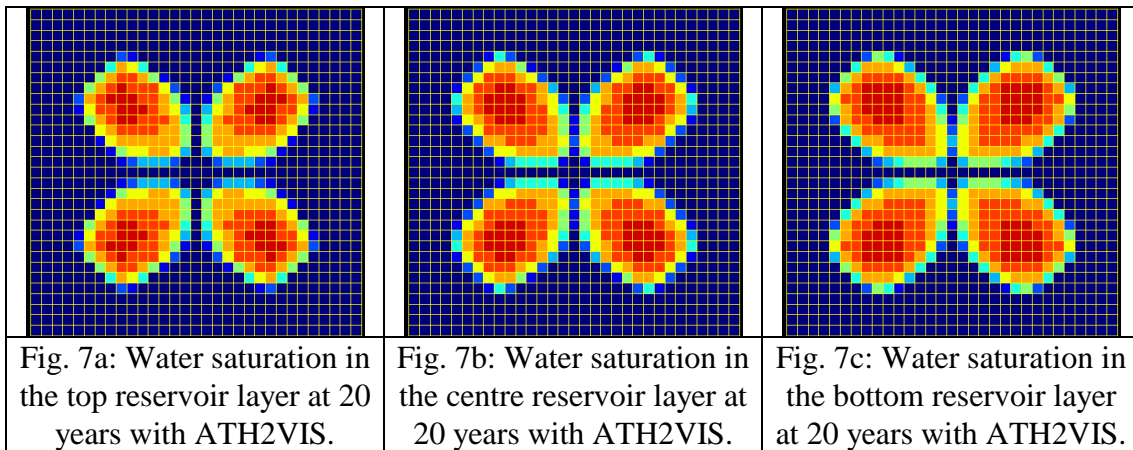
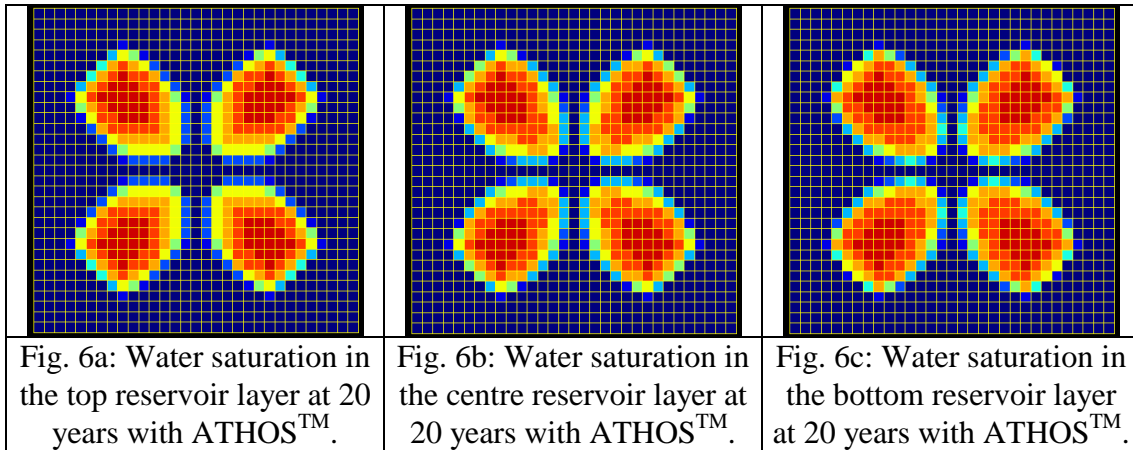


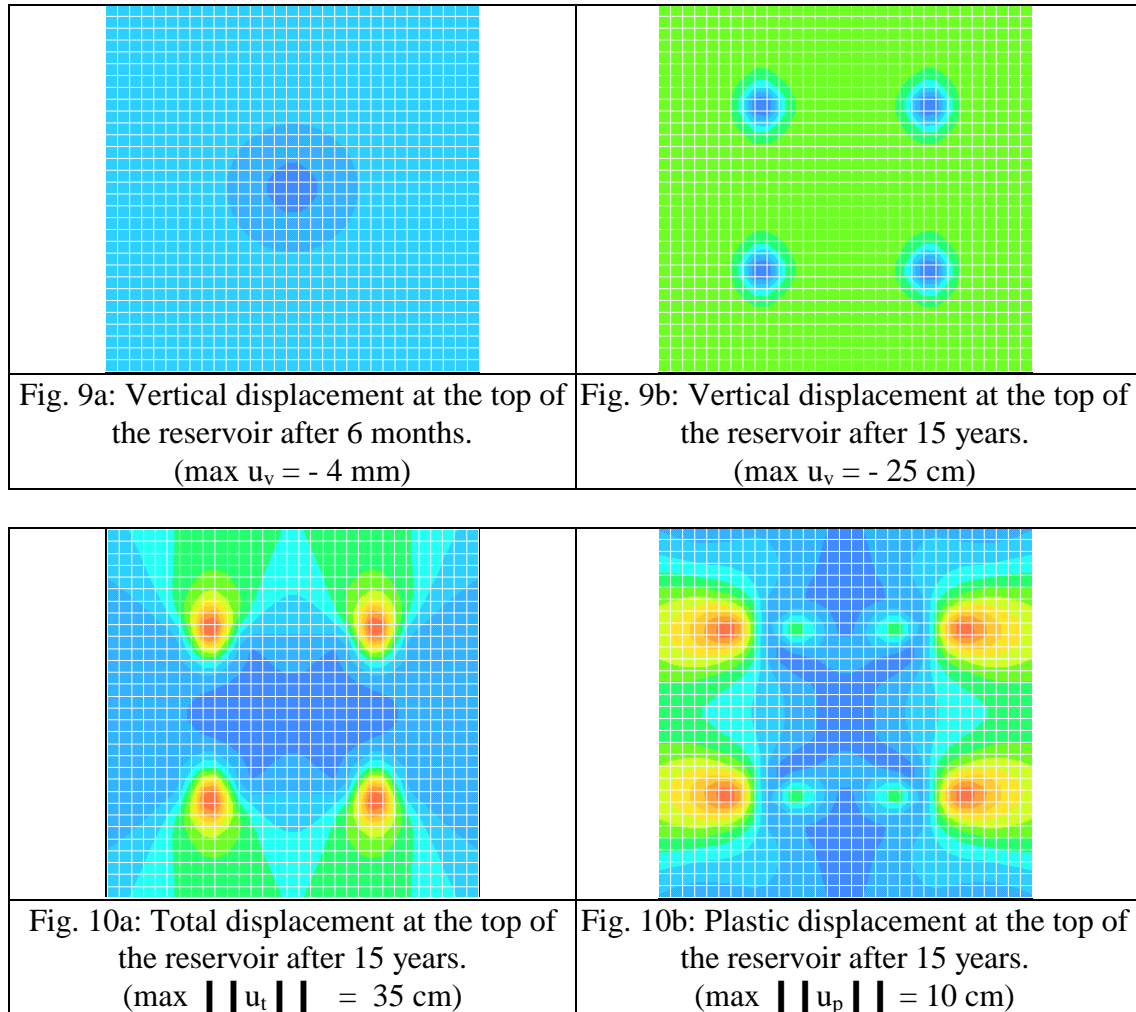
Fig. 4 and 5 compare the reservoir simulation (ATHOS™) with the reservoir stress dependent simulation realised with ATH2VIS. In both cases, production stops when producer bottom hole pressure reaches its threshold value, however this time arises first for the partially coupled simulation compared to the standard simulation. Fig. 5 shows that the difference in breakthrough times is about 1.5 year. This result agrees with the water saturation profiles obtained with both simulators after 20 years of production (see Fig. 6 and 7). The comparison of the water saturation maps shows for each reservoir layer, a larger water propagation towards the centre producer for the permeability stress dependent simulator. For ATHOS™ simulation and as physically expected, there is no favoured directional flow of water in the reservoir. On the contrary, Fig. 7 emphasises that the water flow in the x-direction is slightly larger than the one in the y-direction.

The fast sweeping predicted by the permeability stress dependent simulator can only be attributed to the change in permeability computed by the mechanical simulator. Fig. 8 displays stress dependent permeability in x, y and z-directions after 15 years of production. Permeability change area appears to be the same for all directions and is slightly more lying in the x-direction than in the y-direction. Nevertheless, the magnitude in permeability change greatly depends on the directions with a maximal permeability enhancement of 15 in the x-direction to be compared with permeability enhancement of 45 and 60 in the y and z directions. The higher permeability enhancement in the y and z directions has to be attributed to the fracture directions allowing larger strains in the vertical and fracture directions and lower strains in the normal direction of the fractures.



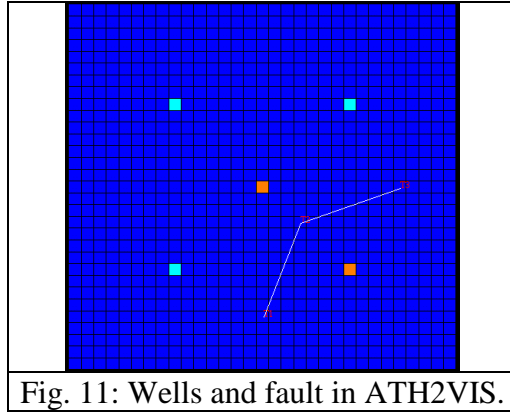
Figures 9 display the vertical displacement at the top of the reservoir during the reservoir depletion period (after 6 months) and during the depletion-injection period (after 20 years). Fig 9a shows a weak compaction at the reservoir centre induced by the reservoir depletion. Furthermore, cold water injection also leads to a non-positive displacement (with a maximal displacement of - 25 cm located at injector well positions) at the reservoir top in spite of the water injection. This result comes from the thermal contraction associated with the cold water arrival and which prevails on the hydro-mechanical effect that would be associated with the pressure increase at the injector well location.

Finally, Figs. 10.a and 10.b present the total and plastic components of the displacement at the top of the reservoir after 15 years. The total displacement is maximal at the injector well locations due to the thermal effect, and horizontal displacements are maximal in the y-direction of the initial horizontal maximal stress. On the contrary plastic displacements are mainly oriented in the x-direction, and higher plastic displacement zones are aligned with the wells in the x-direction. This last result may explain the favoured x-direction of permeability enhancement observed in Fig. 8.

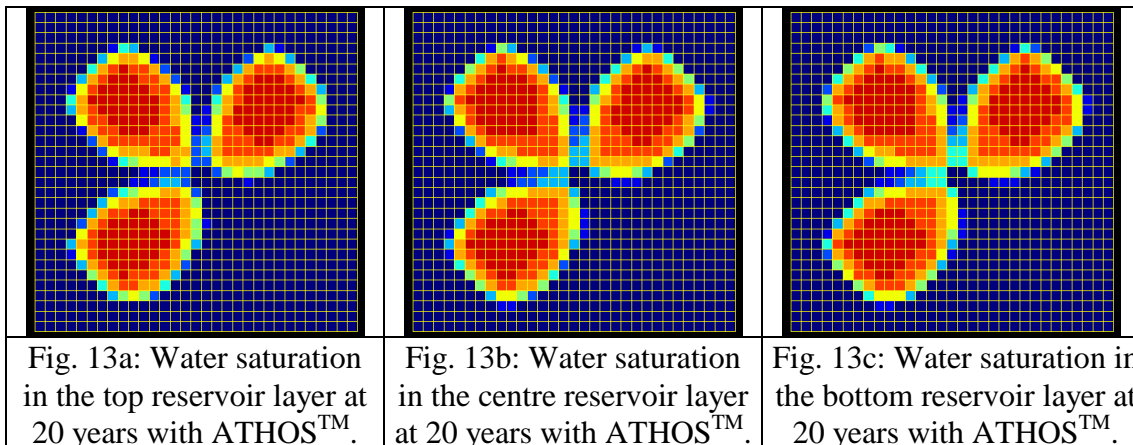
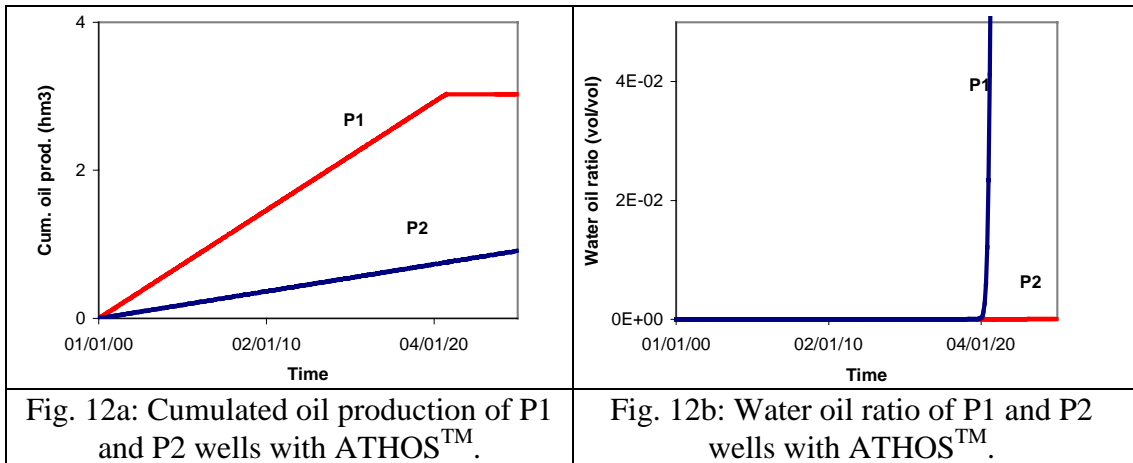


### Role of fault:

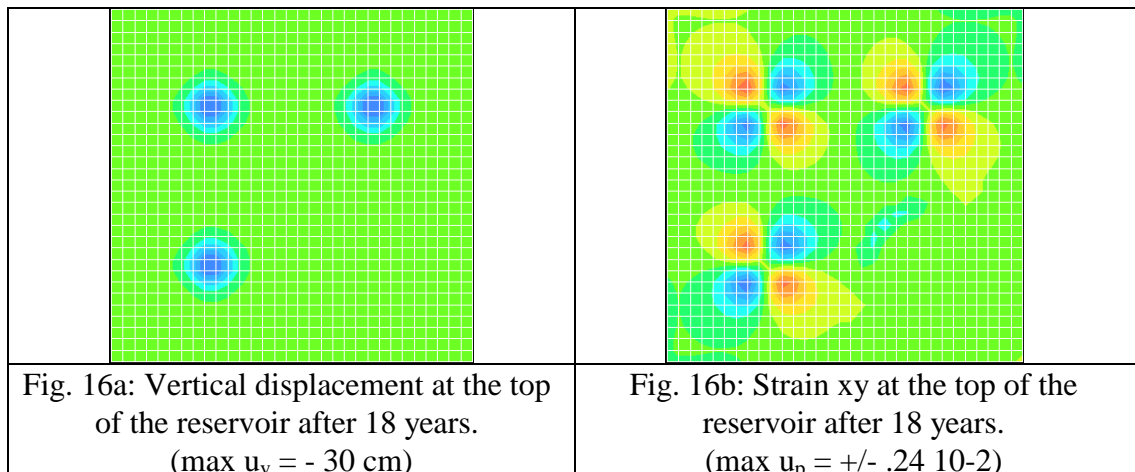
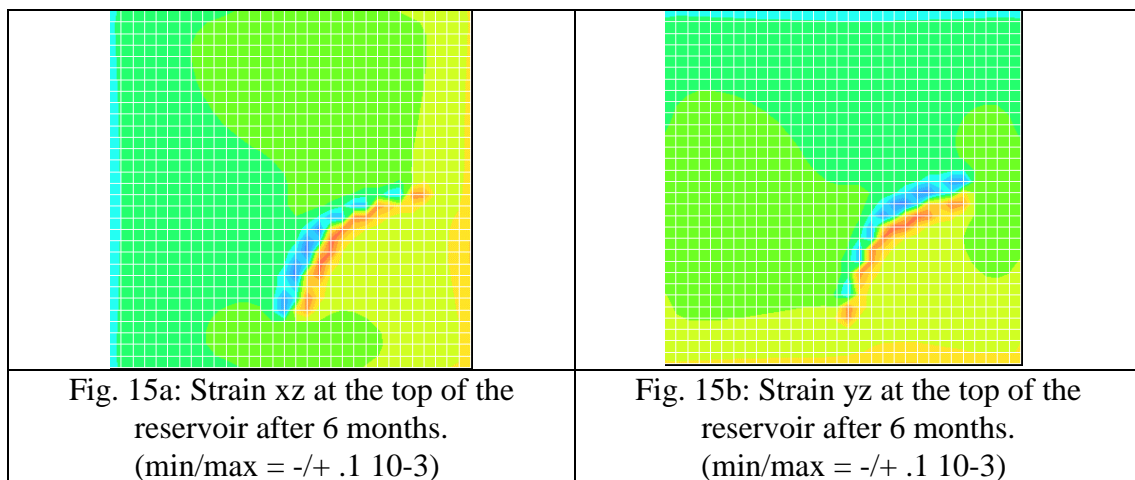
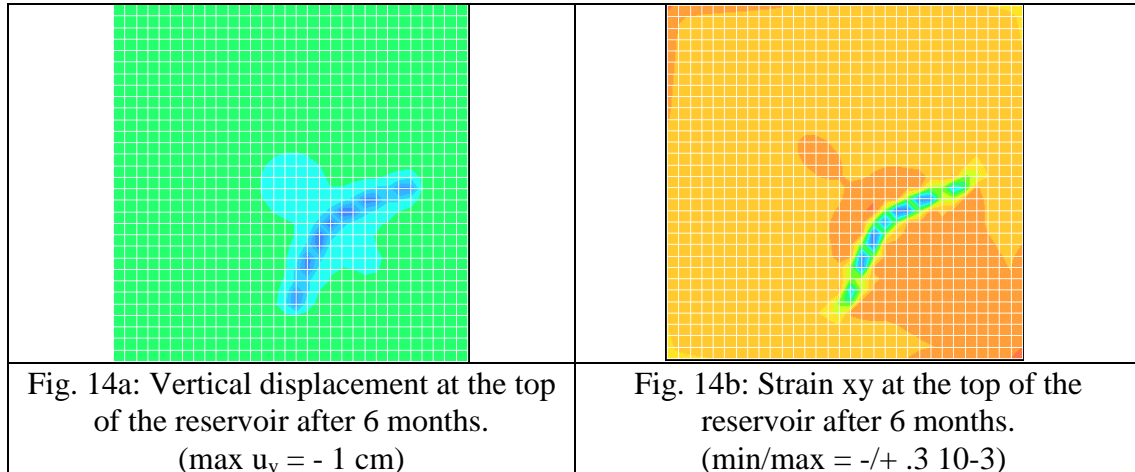
Let us now study the effect of a vertical fault of reduced permeability on reservoir flows and on the reservoir mechanical behaviour. Fault is displayed on Fig. 11. On the reservoir side, permeability of reservoir cells crossed with the fault in direction x, y and z is initialised with reservoir permeability in the same direction divided by  $10^{-4}$ . On the mechanical side, fault mechanical properties are given in Table 4. Fig. 11 also displays well location: a well producer is still located at the centre of the reservoir, however, a new producer well is added on the other side of the fault instead of an injector well for the simulations realised on a fractured reservoir. The production scenario is not changed from the previous case: one year of natural depletion following by a depletion-injection period. The total flow rate (oil + water) in surface condition of the centre producer well P1 now equals 400 m<sup>3</sup>/d whereas the flow rate of the other producer P2 is fixed to 100 m<sup>3</sup>/d. Injectors wells I1, I2, and I3 inject water after one years of production at a flow rate fixed to 170 m<sup>3</sup>/d at surface condition.



Figs. 12 display production results for producer wells P1 and P2 obtained with the reservoir simulator ATHOS<sup>TM</sup>. Producer well P1 closes after 20 years of production when the bottom hole pressure reaches the limit pressure of 70 bar. This time corresponds to the water breakthrough (see Fig. 12b) with the water reaching the centre of the reservoir as it appears on Fig. 13. Simulation performed with the stress dependent simulator ATH2VIS provides no permeability change and then exactly the same productivity results as for ATHOS<sup>TM</sup> simulation (i.e. Figs. 12 and 13 are the same for ATHOS<sup>TM</sup> and ATH2VIS). This result emphasises that for the present simulation the loading of the fault is too low to create fracturing and then permeability change. Other simulations not presented in the paper show that even when fracturing induced through faults occurs, the permeability change does not significantly alter the reservoir productivity due to the very low fault permeability in comparison with reservoir initial permeability.



Figs. 14 to 16 present mechanical effects induced by the reservoir production. The effect of the fault appears on Figs. 14-15 after 6 months of reservoir depletion, and when the water injection has not started. Fig. 14a displays the reservoir vertical displacement that is maximal around the fault and Figs. 14b and 15 display the horizontal shear strain and the xz and yz shear strains. The shear strain is maximal for the horizontal component (i.e. xy). In the present case, shear strains are not significantly large, but sufficient to induce a threat to well integrity. Finally we note that for large values of time, thermal effects associated with the cold water injection are more dominant than mechanical effects induced by the fault (see Fig. 16). Thus the vertical displacement (see Fig. 16a) and the horizontal shear strain (see Fig 16b) around the fault can be neglected with the respective quantities around the injector wells.



## Conclusions:

The paper presents a new stress dependent reservoir simulator ATH2VIS that makes the coupling of the reservoir simulator ATHOS™ with the stress simulator VISAGE™. ATH2VIS is a partially coupled simulator that accounts for permeability variations due to activation of fractures and faults together with rock failure. Two simulation cases are presented for a reservoir of idealised rectangular geometry, with a dead-oil and heat transfer. The first simulation case uses joint sets whereas the second one is realised with a fault of reduced permeability. For both cases, the intact rock failure is prevented in order to primarily analyse the effect of fractures and faults on reservoir flows and the reservoir stress state.

The first scenario considering fractures in the reservoir reveals significant variations of the permeability around water injection wells. Change in permeability is more marked in the y and z directions (closed to the fracture plane directions) and is slightly aligned in the x direction around the cold water injectors. Permeability enhancement induces a faster water infiltration and then an earlier production stop when compared to the prediction of the standard reservoir simulator. On the contrary, the second simulation case including a fault in the reservoir shows no effect on the reservoir flow due to no fault activation. Furthermore, with the very low initial permeability of the fault, it is very difficult for the fault to modify the reservoir productivity. Finally, the effect of the fault appears to be more on the stress state around the fault, and may cause a threat to well integrity.

Next developments of the ATH2VIS simulator will concern reservoir porosity update with a stress dependent porosity for the analysis of compaction and subsidence problems.

## References

- Chin, L.Y., Raghavan, R., and Thomas, L.K. (1998). Fully-Coupled Geomechanics and Fluid-Flow Analysis of Wells with Stress-Dependent Permeability. SPE International Conference and Exhibition in China held in Beijing, China, 2-6 Nov. 269-284
- Chin, L.Y., and, Thomas, L.K. (1999). Fully Coupled Analysis of Improved Oil Recovery by Reservoir Compaction. SPE Annual Technical Conference and Exhibition held in Houston, Texas, 3-6 October. 393-401
- Gutierrez, M., and Makurat, A. (1997). Coupled HTH Modelling of Cold Water Injection in Fractured Hydrocarbon reservoirs. Int. J. Rock Mech. & Min. Sci. 34:3-4, paper No; 113.
- Koutsabeloulis, N., Heffer, K.J., and, Wong, S. (1994). Numerical geomechanics in reservoir engineering. Computer Methods and Advances in Geomechanics, 2097-2104
- Koutsabeloulis, N., and, Hope, S. (1998). Coupled Stress/Fluid/Thermal Multi-Phase Reservoir Simulation Studies Incorporating Rock Mechanics. SPE/ISRM Eurock'98 Conference held in Trondheim, Norway, 8-10 July, 449-454
- Pande, G.N. (1980). Numerical simulation of rock behaviour: problems and possibilities. Numerical Methods in Geomechanics, Vol. 4, 1341-1356
- Settari, A., and, Mourits, F.M., (1994). Coupling of geomechanics and reservoir simulation models. Computer Methods and Advances in Geomechanics, 2151-2158